

Available online at www.sciencedirect.com

Resuscitation

journal homepage: www.elsevier.com/locate/resuscitation

Clinical paper

Capnography: A support tool for the detection of return of spontaneous circulation in out-of-hospital cardiac arrest



Andoni Elola^{a,*}, Elisabete Aramendi^a, Unai Irusta^a, Erik Alonso^a, Yuanzheng Lu^b, Mary P. Chang^c, Pamela Owens^c, Ahamed H. Idris^c

^a Communications Engineering Department, University of the Basque Country UPV/EHU, 48013 Bilbao, Spain

^b Emergency and Disaster Medicine Center, The Seventh Affiliated Hospital, Sun Yat-sen University, Shenzhen, China

^c Department of Emergency Medicine, University of Texas SouthWestern Medical Center (UTSW), Dallas, United States

Abstract

Background: Automated detection of return of spontaneous circulation (ROSC) is still an unsolved problem during cardiac arrest. Current guidelines recommend the use of capnography, but most automatic methods are based on the analysis of the ECG and thoracic impedance (TI) signals. This study analysed the added value of EtCO₂ for discriminating pulsed (PR) and pulseless (PEA) rhythms and its potential to detect ROSC.

Materials and methods: A total of 426 out-of-hospital cardiac arrest cases, 117 with ROSC and 309 without ROSC, were analysed. First, EtCO₂ values were compared for ROSC and no ROSC cases. Second, 5098 artefact free 3-s long segments were automatically extracted and labelled as PR (3639) or PEA (1459) using the instant of ROSC annotated by the clinician on scene as gold standard. Machine learning classifiers were designed using features obtained from the ECG, TI and the EtCO₂ value. Third, the cases were retrospectively analysed using the classifier to discriminate cases with and without ROSC.

Results: EtCO₂ values increased significantly from 41 mmHg 3-min before ROSC to 57 mmHg 1-min after ROSC, and EtCO₂ was significantly larger for PR than for PEA, 46 mmHg/20 mmHg ($p < 0.05$). Adding EtCO₂ to the machine learning models increased their area under the curve (AUC) by over 2 percentage points. The combination of ECG, TI and EtCO₂ had an AUC for the detection of pulse of 0.92. Finally, the retrospective analysis showed a sensitivity and specificity of 96.6% and 94.5% for the detection of ROSC and no-ROSC cases, respectively.

Conclusion: Adding EtCO₂ improves the performance of automatic algorithms for pulse detection based on ECG and TI. These algorithms can be used to identify pulse on site, and to retrospectively identify cases with ROSC.

Keywords: Return of spontaneous circulation (ROSC), ROSC detection, Capnography, End-tidal CO₂ (EtCO₂), Electrocardiogram (ECG), Thoracic impedance

1 Introduction

The main goal of resuscitative efforts during out-of-hospital cardiac arrest (OHCA) is to achieve return of spontaneous circulation (ROSC). Those efforts include high quality cardiopulmonary resuscitation

(CPR), during which chest compressions should be minimally interrupted for actions like rhythm analysis or pulse checks. Current pulse detection methods such as carotid pulse check, or checking for signs of life as recommended by the current guidelines, are both time consuming and inaccurate.^{1–5} There is therefore a need for accurate and automated pulse detection methods⁶ that can be used by

* Corresponding author.

E-mail address: andoni.elola@ehu.es (A. Elola).

<https://doi.org/10.1016/j.resuscitation.2019.03.048>

Received 10 December 2018; Received in revised form 27 February 2019; Accepted 18 March 2019

0300-9572/© 2019 Elsevier B.V. All rights reserved.

emergency medical personnel as a decision support tool to identify ROSC. Such methods would contribute to improve therapy, reduce and shorten pauses in chest compressions, and increase survival rates.^{7,8}

Current guidelines support the use of capnography for early detection of ROSC.⁹ Higher values of end tidal CO₂ (EtCO₂), and sudden increases in EtCO₂ have been linked to ROSC in OHCA.^{10–13} Although some medical algorithms exist for the detection of ROSC using EtCO₂ values,¹⁴ the only automatic method based on capnography was recently proposed.¹⁵

Most automatic methods for the detection of pulse in OHCA rest on the analysis of the ECG and the thoracic impedance (TI). The TI signal shows low amplitude fluctuations for every effective heartbeat,¹⁶ so features characterizing the TI signal have been proposed alone,^{17–19} or in combination with ECG features^{20–22} for the detection of pulse. In this context, detection of pulse is framed as a classification problem with two types of organized rhythms: pulse-generating rhythms (PR) and pulseless electrical activity (PEA).

The purpose of this study was to evaluate the added value of capnography for the classification of PR/PEA during OHCA. First, EtCO₂ values were automatically detected in order to compare the values between patients with and without ROSC, and to analyse how EtCO₂ changed as the patient approached ROSC. Then, the added value of EtCO₂ for PR/PEA classification was evaluated by developing machine learning PR/PEA classifiers.

2 Materials

For this study we analysed 1561 OHCA episodes retrospectively, treated by the Dallas FortWorth Center for Resuscitation Research (UTSW, Dallas) using the Philips HeartStart MRx device between 2012 and 2016. The device files included the ECG and TI recorded through the defibrillation pads with sampling frequencies of 250 Hz/200 Hz respectively, and capnography recorded through sidestream acquisition with a sampling frequency of 125 Hz. The electronic files were linked to clinical annotations and ROSC was defined as palpable pulse in any vessel for any length of time. The first ROSC instant annotated by the rescuer on scene was the gold standard; based on that instant PR and PEA annotations were made automatically and patients with ROSC and without ROSC were classified.

The following patient inclusion/exclusion criteria were applied. Only episodes with TI, ECG and capnography were considered ($n=835$). Cases where ROSC was suspected but not annotated by clinicians on site were excluded, which comprised patients transported to hospital ($n=252$), or episodes with long periods (>2 min) without compressions presenting an organized rhythm with EtCO₂ above 25 mmHg ($n=26$). Episodes with suspected intermittent ROSC were also excluded, these were episodes in which shocks or chest compressions (>2 min) were delivered after the annotated onset of ROSC ($n=76$). For our analysis of the ROSC cases, the capnogram had to be available at least 4 min before and 1 min after the onset of ROSC. If not, the case was excluded ($n=55$). The final dataset contained 426 episodes, 117 with ROSC and 309 without ROSC. Fig. 1 shows a 3-min interval from two cases of the study dataset. In the ROSC case (top panel) EtCO₂ increases at ROSC onset, and after ROSC the heart rate increases and there is pulse related activity in the TI. In the no-ROSC case (bottom panel) EtCO₂ is always below 20 mmHg, and although the heart rate changes during PEA there is no pulse related activity in the TI.

3 Methods

Three analyses were conducted: EtCO₂ levels in episodes with and without ROSC, development and evaluation of a PR/PEA classifier using ECG/TI segments and EtCO₂ values, and a case study of the use of the classifier to retrospectively identify cases as ROSC/no-ROSC.

3.1 Analysis of EtCO₂ levels

Onset and offset of each ventilation were automatically delineated in the capnogram using a method introduced in a previous study.²³ For each ventilation, EtCO₂ was automatically calculated as the maximum CO₂ value during the alveolar plateau (see Fig. 1).

In ROSC cases, median EtCO₂ levels were computed every minute (MEtCO₂) in a 5 min interval around ROSC (4-min before to 1-min after). Similarly, for patients without ROSC, the MEtCO₂ values were computed for each one of the last 5 min of the episode. The MEtCO₂ value for the last minute of the episode corresponds to the last minute before the EOE, i.e. the instant when the monitor/defibrillator was disconnected.

3.2 PR/PEA machine learning classifier

Following the classical scheme proposed in previous studies,^{22,20,21} the detection of ROSC implies the discrimination between PR and PEA once an organized rhythm is identified by the shock advice algorithm. It is therefore a two class classification problem, for which, first, the dataset of PR/PEA segments was defined, and then a classifier was designed using features extracted from the ECG, TI and capnography signals.

3.2.1 PR/PEA segment dataset

PR and PEA segments of 3.2-s duration were extracted during intervals with no chest compression artefacts. Pauses in chest compressions were automatically detected using the compression depth signal from the CPR assist pad when available,²⁴ or the TI otherwise.²⁵ Segments with large ECG amplitude oscillations (>3.5 mV) were discarded as noisy, and then organized rhythms (PEA or PR) were detected during the pauses using an offline version of a rhythm analysis algorithm of a commercial automated external defibrillator (AED).²⁶ In ROSC cases, all segments before ROSC onset were labelled as PEA, and those after ROSC onset as PR (see Fig. 1, panel a). In no-ROSC cases, all segments were labelled as PEA (see Fig. 1, panel b). A minimum separation between consecutive segments of 20-s was enforced to foster ECG and TI waveform diversity in the segments.

3.2.2 Machine learning PR/PEA classifier

Nine PR/PEA classification features were computed from the most recently proposed algorithms, six ECG features introduced in Ref.²⁷ and three TI features.^{22,17,28} These ECG and TI features are described in detail in Appendix A. The MEtCO₂, the median EtCO₂ in the minute before the analysis window (pause in chest compressions with organized ECG rhythm) was also added. The features were combined in a Random Forest (RF) classifier, a machine learning algorithm based on the aggregate vote of several independently designed uncorrelated decision trees.²⁹ RF classifiers

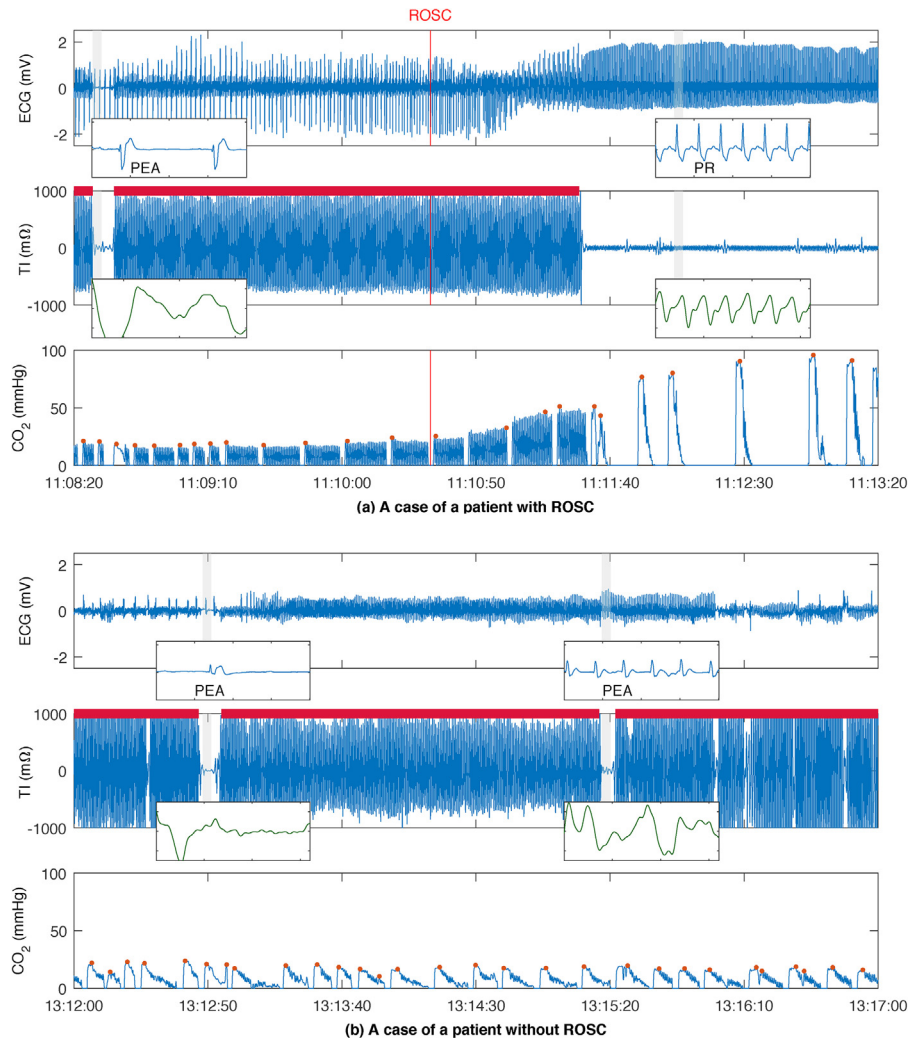


Fig. 1 – ECG, Thoracic Impedance (TI) and capnography signals for a patient with ROSC, panel (a), and without ROSC, panel (b). ROSC onset, as annotated by a clinician on site, is represented by a red line in the first example. The extracted 3.2-s segments are shaded in grey and the ECG and TI (green) are zoomed in. Chest compression intervals are depicted above TI signal. In the ROSC case a PEA and a PR segments were extracted in the depicted interval, and two PEA segments in the no-ROSC case. Ventilations were automatically detected in the CO₂ curve, and the automatically measured EtCO₂ value is highlighted with red dots. In the ROSC case after pulse recovery the ECG presents stable and normal QRS complexes and heart rate, and chest compressions are stopped so there is no activity in the impedance.

have shown excellent performance in many classification problems, including PR/PEA classification,²⁷ and are robust against annotation errors.

All patients were weighted equally to train the RF classifier and 300 trees were used. For each segment, the RF classifier computes the probability of being PR (p_{pr}), and segments were classified as PR for $p_{pr} > 0.5$ and as PEA otherwise. The classifier was trained and tested using a patient wise 10-fold cross-validation procedure.³⁰ For each of the 10 folds, the algorithm was optimized using 90% of the cases, and the accuracy results were obtained from the remaining 10% (test fold). This procedure guaranteed that the optimization of the classifier and the estimation of its accuracy were done on data from separate patients, and that the performance was assessed using all available data.

3.3 Case study: retrospective identification of patients with ROSC

Using the PR/PEA classifier, a simple method was developed to automatically identify patients with ROSC in a retrospective analysis of a set of OHCA episodes. This method may be used as an automated tool for post arrest debriefing or annotation. Complete episodes (until EOE) were processed and the case was labelled as ROSC if from any three consecutive segments at least two were identified as PR by the classifier.

Our ground truth was the ROSC instant annotated by clinicians on scene, which discriminated the group of patients with ROSC and patients without ROSC, and the detection of episodes with ROSC was evaluated using the test sets in the 10-fold cross validation procedure.

3.4 Statistical analysis

MEtCO₂ distributions did not pass the Kolmogorov–Smirnov normality test, and are reported as median and interquartile range (IQR). MEtCO₂ distributions at different times (within ROSC cases) or between ROSC/no-ROSC cases were compared using the Mann–Whitney *U* test. Differences were considered significant for $p < 0.05$.

PR/PEA classification was evaluated using Receiver Operating Characteristic (ROC) curves, and the area under the curve (AUC) was used as measure of performance.³¹ The Youden index was used to define the optimal point in the ROC curve, which gives equal importance to the sensitivity (SE, for PR segments) and specificity (SP, for PEA segments).³²

When the classifier was used as a retrospective tool to identify ROSC, SE and SP were defined as the proportion of correctly identified ROSC and no-ROSC cases, respectively.

4 Results

The mean (standard deviation) durations were 58 (23) min and 38 (11) min for the episodes with and without ROSC, respectively. The commercial AED algorithm detected 5098 segments with organized rhythms. A total of 3639 PR segments were extracted from episodes with ROSC, and 1459 PEA segments, 308 from episodes with ROSC and 1151 from episodes without ROSC. Some examples of the extracted ECG segments can be found in Figs. 1 and 4. The median (IQR) ventilation rate per episode was 7.8 (5.7–10.5) min⁻¹.

The MEtCO₂ for ROSC cases were statistically significantly larger than for no-ROSC cases at all time-stamps (Fig. 2). Elevated EtCO₂ levels were observed in patients with ROSC, with an upward trend from 41 mmHg (at 3 min before ROSC) to 57 mmHg close to ROSC onset (see Fig. 2a).

Fig. 3 shows the ROC curves of the RF classifier for different features sets. The curves in panel (a) were calculated using the whole dataset, while the curves in panel (b) were calculated excluding the

PEA segments extracted from patients with ROSC, that is the pre-ROSC PEA segments. The analysis of the ROC curves is shown in Table 1. The ROC curves showed that the AUC of the PR/PEA classifier increased as features from different sources were added. Including MEtCO₂ in the classifier increased the AUC for all feature combinations, thanks to the added uncorrelated information. Adding MEtCO₂ to an ECG-only and to an ECG+TI based classifiers increased their AUCs in 3 and 2-points, respectively. The best classifier combined all features and presented an AUC of 0.92 with a SE and SP of 84% and 86%, respectively (see Table 1). MEtCO₂ alone was also a good classifier (AUC around 0.76), the median MEtCO₂ values were 46 (32–64) mmHg for PR and 20 (8–38) mmHg for PEA segments ($p < 0.05$).

The accuracy of the classifiers increased when PEAs that transitioned to PR (episodes with ROSC) were not included. The accuracy increase was on average 4-points for all classifiers (see Table 1). Significant differences were observed between PEAs in ROSC and no-ROSC cases. The MEtCO₂ values of the PEA in the ROSC and no-ROSC cases were 31 (20–44) mmHg and 16 (7–35) mmHg ($p < 0.05$), respectively. The probabilities of being PR, p_{pr} , for the classifier with all features were also significantly different for these two subgroups of PEA, 0.09 (0.03–0.29) for the PEA from no-ROSC cases and 0.33 (0.11–0.58) for those of the ROSC cases ($p < 0.05$).

Fig. 4 shows the performance of the PR/PEA classifier with three consecutive segments in three patients. Each panel represents the 3 consecutive 3.2-s ECG and TI segments used for analysis, and the capnogram in the 1-min interval before the segment, which was used to compute MEtCO₂ (depicted as a dashed line). The text on top of each segment shows the true class followed by the class predicted by the classifier. The first example (panel a) shows a patient achieving ROSC transitioning from PEA to PR in which all segments were correctly classified. The first segment was taken 80 s prior to ROSC (PEA) and the other two after ROSC. It can be observed that heart rate, TI activity and MEtCO₂ (specially in PEA/PR transition) increase among consecutive segments. The second example (panel b) shows three correctly classified PEA segments in a patient without ROSC.

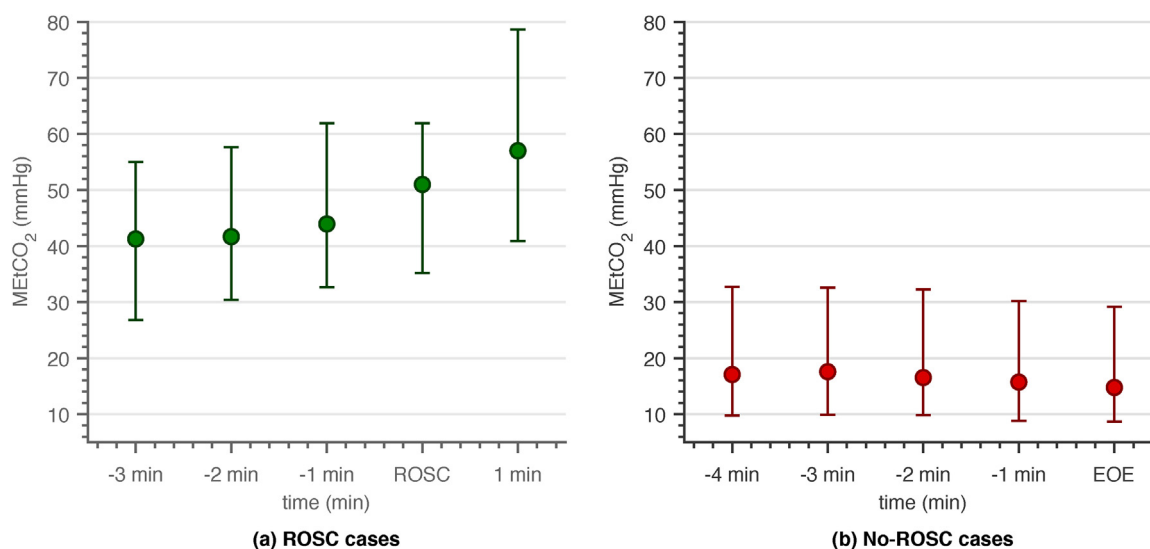


Fig. 2– Median EtCO₂ (MEtCO₂) values and their interquartile ranges for cases with ROSC (left) and no-ROSC (right). For ROSC cases the interval around ROSC onset is analysed, in the no-ROSC cases the 5 min before the end of episode (EOE) are shown. MEtCO₂ was calculated as the median EtCO₂ value of all ventilations in a 1-min interval before the indicated time-stamp.

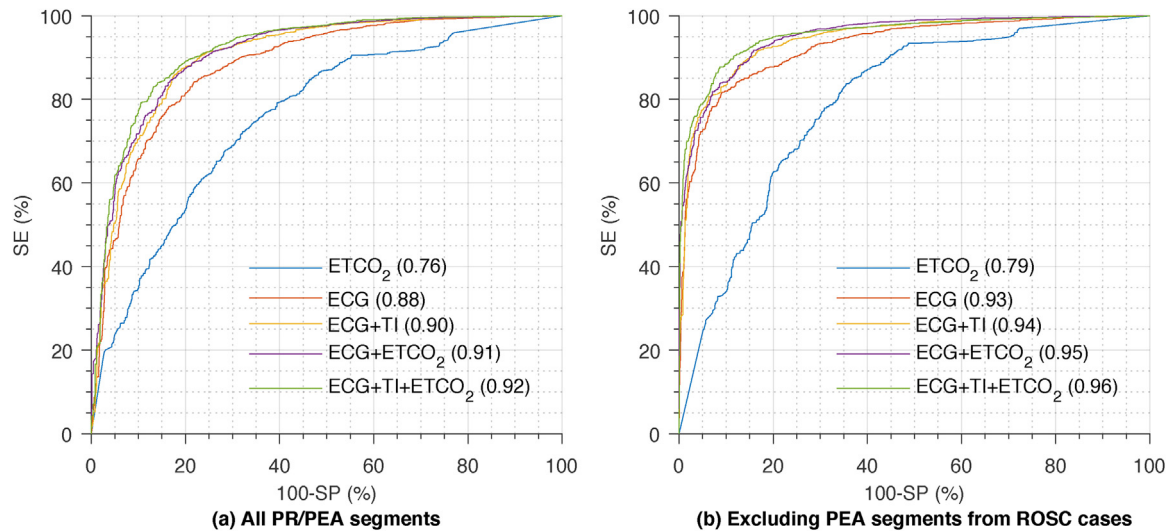


Fig. 3 – ROC curves of the RF classifier for different feature sets. Panel (a) shows results for the whole dataset, while panel (b) shows the curves after excluding the PEAs from episodes with ROSC. The AUC value for each classifier is shown between parentheses.

Table 1 – ROC curve analysis of the machine learning classifier when the whole PR/PEA dataset is considered and when the PEAs from ROSC cases were excluded. The SE and SP are given for the optimal point according to the Youden index.

	All PR/PEA segments			Excluding PEAs from ROSC		
	AUC	SE	SP	AUC	SE	SP
EtCO ₂	0.76	72.3	67.8	0.79	83.7	64.6
ECG	0.88	84.2	78.2	0.93	81.7	90.8
ECG+TI	0.90	86.7	81.6	0.94	88.4	87.0
ECG+EtCO ₂	0.91	86.3	81.5	0.95	91.8	84.2
ECG+TI+EtCO ₂	0.92	83.9	86.0	0.96	87.8	91.3

Despite having a heart rate above 60 bpm, low EtCO₂ values and low circulation-related TI activity yielded the correct classification of the three segments and of the patient without ROSC. The third example, however, corresponds to a patient without ROSC incorrectly identified as patient with ROSC. Two of the segments were classified as PR because the ECG was regular with a heart rate above 60 bpm, the TI showed large fluctuations and EtCO₂ levels were above 30 mmHg.

When the PR/PEA classifier with all features was used as a retrospective tool to automatically identify episodes with and without ROSC, the SE and SP were 96.6% and 94.5%, respectively. Only 4 cases with ROSC were misidentified as no-ROSC, and 17 cases with no-ROSC were identified as ROSC cases.

5 Discussion

Detection of ROSC remains a challenge in OHCA, and there is still a need for a reliable monitoring of the hemodynamic state of the patient.⁶ This study shows that EtCO₂ has great potential to support the rescuer in the identification of ROSC, both as a stand-alone marker but also in combination with the ECG and TI. This is, to the best of our knowledge, the first study that demonstrates that the addition of EtCO₂ improves PR/PEA classification based on the ECG or on the combination of ECG and TI.

The results shown in Fig. 2 and Table 1 reveal that a three-signal classifier provides better performance than two-signal solutions, which are better than a classifier based on a single signal. These results may help in the design of PR/PEA classification systems, and different solutions may be implemented depending on the availability or usability of the signals in a particular monitor/defibrillator.

For this study, we extracted PEA segments from patients with and without ROSC, and we relied on the ROSC onset annotations made by clinicians on site. We believe that is the most realistic (and challenging) scenario, although we observed differences in the characteristics of the PEA obtained from patients that ultimately recovered ROSC and those who did not. MEtCO₂ levels during PEA were significantly higher in patients that recovered ROSC, and the AUCs of the PR/PEA classifiers increased by over 4-points when PEAs from patients that recovered ROSC were not included. In fact, the SP for the PEAs of the patients that recovered ROSC was 61.2%, significantly lower than 91.2% obtained for the patients with no ROSC. There are two main reasons behind the differences in SP. First, the instant of ROSC annotated by clinician on scene and used as gold standard might show some delay depending on the rescuer. Second, there are differences between PEAs leading to PR (from ROSC patients) and PEAs not leading to PR (from patients without ROSC). Rhythms from first group are more likely to be pseudo-PEAs since they present a better prognosis, and they show different ECG

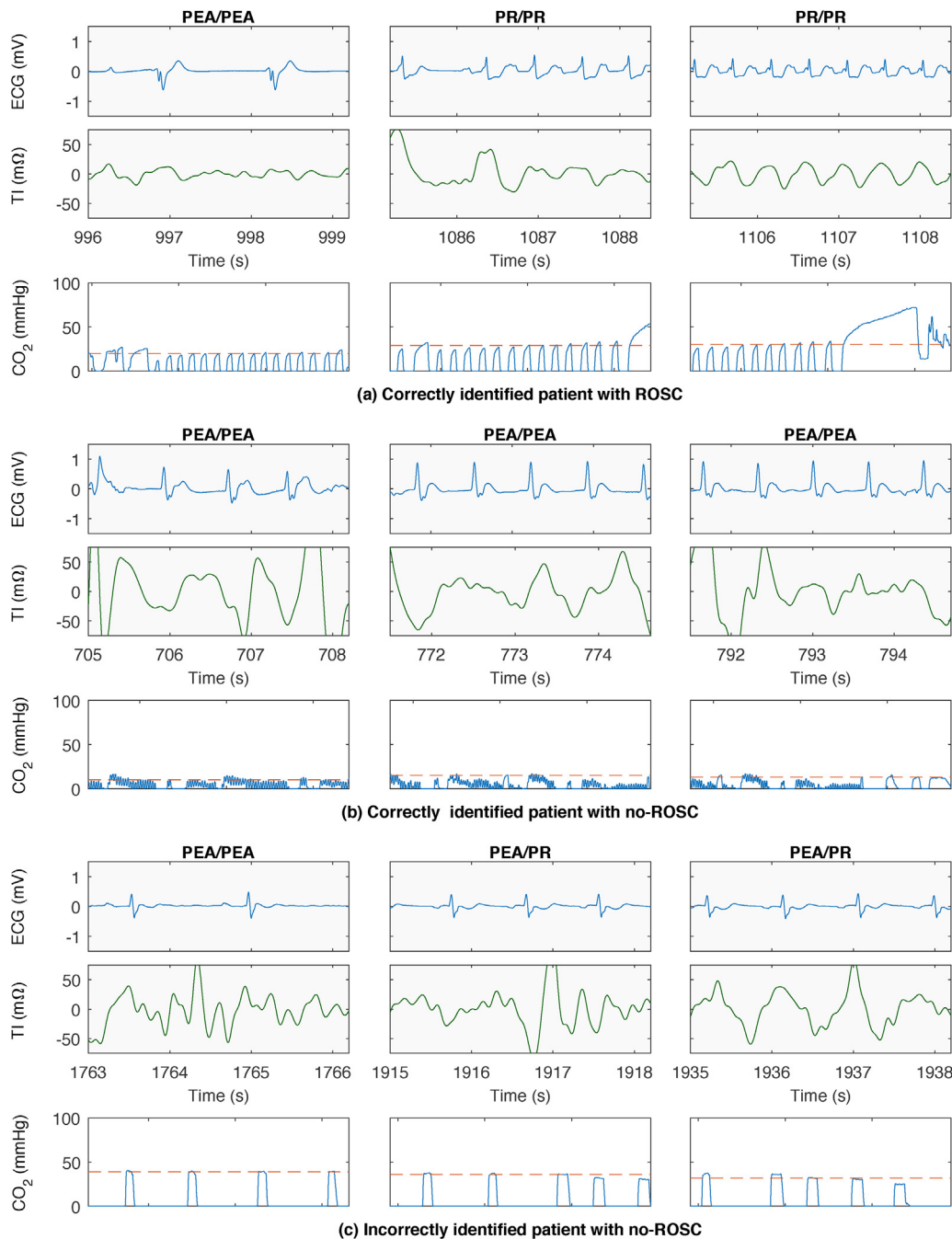


Fig. 4 – Examples of the case study. Panels (a), (b) and (c) show a correctly identified patient with ROSC, a correctly identified patient without ROSC, and a patient without ROSC incorrectly identified, respectively. Each panel depicts the three consecutive PEA/PR segments analysed. The text on top of each segment indicates its true label followed by the predicted label by the classifier. The capnogram corresponds to the minute before the onset of the segment and the dashed horizontal line represents the $MEtCO_2$.

characteristics and $EtCO_2$ values.^{33–39} This type of border rhythm challenges the design of an accurate classifier. An experiment supporting these conclusions is detailed in the supplementary file. The p_{pr} obtained from the classifier was significantly lower for PEA in no-ROSC cases, and as shown in Fig. 5, the median value of p_{pr} increases for PEA in ROSC patients as the patient approaches ROSC onset. This indicates that the p_{pr} obtained from the RF classifier may

serve as a potential surrogate hemodynamic marker that could measure the evolution of PEA in response to therapy.

The analysis of the $MEtCO_2$ values for the intervals around ROSC (Fig. 2a) showed that $EtCO_2$ values increase as the patient approaches ROSC, and the rise is higher closer to ROSC onset, in line with previous findings.^{12,13} We also observed that $EtCO_2$ levels were maintained after ROSC, or even decreased if ventilation rates

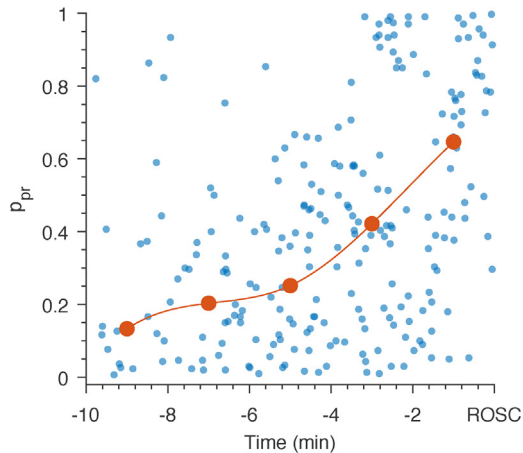


Fig. 5 – Time evolution of p_{pr} for the PEA segments as the patients approach ROSC. Blue dots indicate values for each segment, and the red curve is fitted to the median values of p_{pr} every 2 min.

were high. Abrupt increases in EtCO₂ can be used to identify ROSC onset, but are of little use in a PR/PEA classifier due to its short period utility time. During both PR and PEA, EtCO₂ may increase or decrease around high (PR) or low (PEA) baseline levels. However, interrupting chest compressions only after a sudden increase in EtCO₂ to check for an organized rhythm facilitate early detection of ROSC and minimize hands-off intervals by avoiding unnecessary chest compressions pauses to check for pulse.^{9,14} The EtCO₂ levels reported in this study were high, which may be caused by the inclusion criteria applied to the data that contained those patients with sustained ROSC.

The overall performance of the PR/PEA discriminator is high (AUC > 0.9), but slightly below the scores reported by other methods based exclusively on the ECG²⁷ or combination of ECG and TI.^{21,22} Those studies used segments selected ad-hoc for the processing of the ECG or the TI, which might have introduced a positive bias in the results. Our dataset was automatically selected, including all segments classified as organized rhythm by a commercial AED algorithm, and segment labelling was based exclusively on ROSC annotations made by clinicians on site. In fact, when we applied the method proposed in Ref.²⁷ to the dataset of this study, the SE/SP were 78.8%/84.1%, well below the 88.4%/89.7% reported in the original paper. This dataset reflects a more realistic and difficult scenario for PR/PEA classification.

As an example of applicability of the PR/PEA classifier, a simple automatic tool to retrospectively identify cases with ROSC was proposed. In our 426 cases, a simple method was over 95% accurate, yielding a 96.6% SE and a 94.5% SP for the retrospective detection of ROSC. These values are well above the 73.9% SE and 58.4% SP reported for an automatic algorithm based on capnography trends alone.¹⁵

Finally, the accuracy of the PR/PEA classifier supports its applicability as an automatic decision support tool to aid clinicians in the identification of ROSC. The algorithm uses only a 3.2-s analysis interval without chest compressions, so it can be used during CPR with minimal interruptions to chest compressions. Furthermore, we used an automatic CO₂ based ventilation detector that identifies the offset/onset of ventilations. This allows us to measure the EtCO₂ level as the maximum value during the alveolar plateau in the capnography, which

avoids some of the problems associated with EtCO₂ readings (capnometry) at the end of the expiratory phase when chest compression artefacts are present in the CO₂ waveform.⁴⁰ Each ventilation was delineated using the algorithm proposed in,²³ a software-based algorithm that could be integrated in any equipment without hardware modifications. The algorithm is launched once the AED algorithm has detected an organized rhythm, and it only requires waveform characteristics of the 3.2-s long ECG and TI signals and the median of the EtCO₂ values in the minute prior to the analysis.

6 Limitations

This study shows three limitations. Firstly, the data were collected with the capnography module of the Philips HeartStart MRx monitor/defibrillator. Using another capnometer might alter the levels of EtCO₂. Secondly, our ground truth for all the experiments was the time of ROSC annotated by the clinician on scene. Using an independent gold standard for circulation, such as invasive blood pressure, would result in more robust conclusions. Lastly, there were no data available on the advanced airway technique used on each patient. However, the reported EtCO₂ values might be affected by the used airway management technique (supraglottic/endotracheal).

7 Conclusions

The results of this study demonstrate the added value of the capnogram for the automatic detection of ROSC in OHCA. The EtCO₂ level added discriminative power to the PR/PEA classifier based on the ECG and the TI. The accuracy of the models increased significantly when MEtCO₂ levels were added. This study shows that an automatic algorithm that uses capnography can be implemented to reliably detect ROSC.

Conflict of interest

Dr. Idris receives research grants from the US National Institutes of Health (NIH) and serves as an unpaid volunteer on the American Heart Association National Emergency Cardiovascular Care Committee and the HeartSine, Inc. Clinical Advisory Board.

Acknowledgements

This work has been partially supported by the Spanish Ministerio de Economía y Competitividad, jointly with the Fondo Europeo de Desarrollo Regional (FEDER), project TEC2015-64678-R, by the University of the Basque Country via the Ayudas a Grupos de Investigación GIU17/031, and by the Basque Government through the grant PRE_2017_1_0112.

Appendix A. Signal processing and feature extraction

Nine features (v_1-v_9) were computed from the ECG ($s[n]$) and the TI ($z[n]$) signals. The ECG was filtered between 0.5 Hz and 30 Hz using zero-phase filtering to remove baseline component and high

frequency noise. The TI was resampled to 250 Hz and filtered between 0.7 and 7 Hz to remove fluctuations caused by ventilations and enhance the circulation component.

Six different features, v_1 – v_6 , were calculated from the ECG as recently proposed in²⁷.

- The first difference of the signal ($s_{\Delta} = s[n] - s[n-1]$) was computed and the mean of its absolute value was the first feature:

$$v_1 = \frac{1}{N} \sum_{n=1}^N |s_{\Delta}[n]| \quad (\text{A.1})$$

where N is the length of the segment in samples.

- The standard deviation of $s_{\Delta}[n]$:

$$v_2 = \sqrt{\frac{\sum_{n=0}^{N-2} (s_{\Delta}[n] - v_1)^2}{N-3}} \quad (\text{A.2})$$

- The kurtosis (tailedness) of the square and averaged (with a 125 ms moving average filter) of s_{Δ} was v_3 .
- Amplitude spectrum area (AMSA) is the sum of spectral amplitudes weighted by their frequency components. The spectral amplitudes at f_i, A_i were calculated using the $N_F=4096$ point FFT of the Tuckey windowed $s[n]$ segment:

$$v_4 = \sum_i A_i \cdot f_i, \quad 2 < f_i < 30 \quad (\text{A.3})$$

- The energy of $s[n]$ at frequencies higher than 17.5 Hz:

$$v_5 = \frac{f_s}{2N_F} \sum_i A_i^2, \quad 17.5 < f_i < 30 \quad (\text{A.4})$$

- Fuzzy entropy of $s[n]$, a measure of its regularity, was the v_6 feature.

PEA is defined as absence of palpable pulse when organized electrical activity of the heart is present. The TI signal shows small fluctuations for every effective heartbeat. Many efforts have been made to extract the circulation component of the signal using adaptive filters or ensemble averaging,^{21,20,41} but all of them need accurate QRS detection. Ruiz et al. and Alonso et al. considered the circulation component as a quasi-periodic signal and estimated its Fourier coefficients using least mean squares or recursive least squares algorithms. The instantaneous heart rate was computed from the QRS complexes. Risdal et al. applied ensemble averaging to the TI signal around QRS instants to extract the circulation component. However, in this study we considered only features independent of QRS complex detection, in particular those proposed in^{17,28,22}:

- The mean power of the two half segments of $z[n]$ were computed and the minimum value assigned to v_7 .²²
- The power spectrum of the first difference of $z[n]$ was computed, and v_8 was its peak amplitude in the 1.5–4.5 Hz range.¹⁷
- The normalized cross-correlation function was computed as follows:

$$r_{sz}(l) = \frac{1}{\sqrt{r_{ss}r_{zz}}} \sum_{n=1}^N s[n]z[n-l], \quad l = 0, \pm 1, \dots, \pm N-1 \quad (\text{A.5})$$

where $r_{ss} = \sum_{n=1}^N (s[n])^2$ and $r_{zz} = \sum_{n=1}^N (z[n])^2$. The maximum peak of $r_{sz}[l]$ was v_9 .²⁸

Appendix B. Supplementary data

Supplementary data associated with this article can be found, in the online version, at <https://doi.org/10.1016/j.resuscitation.2019.03.048>.

REFERENCES

1. Perkins GD, Stephenson B, Hulme J, Monsieurs KG. Birmingham assessment of breathing study (BABS). *Resuscitation* 2005;64:109–13.
2. Ruppert M, Reith MW, Widmann JH, et al. Checking for breathing: evaluation of the diagnostic capability of emergency medical services personnel, physicians, medical students, and medical laypersons. *Ann Emerg Med* 1999;34:720–9.
3. Nyman J, Sihvonen M. Cardiopulmonary resuscitation skills in nurses and nursing students. *Resuscitation* 2000;47:179–84.
4. Eberle B, Dick W, Schneider T, Wisser G, Doetsch S, Tzanova I. Checking the carotid pulse check: diagnostic accuracy of first responders in patients with and without a pulse. *Resuscitation* 1996;33:107–16.
5. Ochoa FJ, Ramalle-Gomara E, Carpintero J, Garcia A, Saralegui I. Competence of health professionals to check the carotid pulse. *Resuscitation* 1998;37:173–5.
6. Babbs CF. We still need a real-time hemodynamic monitor for CPR. *Resuscitation* 2013;84:1297–8.
7. Christenson J, Andrusiek D, Everson-Stewart S, et al. Chest compression fraction determines survival in patients with out-of-hospital ventricular fibrillation. *Circulation* 2009;120:1241–7.
8. Berg RA, Sanders AB, Kern KB, et al. Adverse hemodynamic effects of interrupting chest compressions for rescue breathing during cardiopulmonary resuscitation for ventricular fibrillation cardiac arrest. *Circulation* 2001;104:2465–70.
9. Soar J, Nolan JP, Böttiger BW, et al. European resuscitation council guidelines for resuscitation 2015: section 3. Adult advanced life support. *Resuscitation* 2015;95:100–47.
10. Hartmann SM, Farris RW, Di Gennaro JL, Roberts JS. Systematic review and meta-analysis of end-tidal carbon dioxide values associated with return of spontaneous circulation during cardiopulmonary resuscitation. *J Intensive Care Med* 2015;30:426–35.
11. Sheak KR, Wiebe DJ, Leary M, et al. Quantitative relationship between end-tidal carbon dioxide and CPR quality during both in-hospital and out-of-hospital cardiac arrest. *Resuscitation* 2015;89:149–54.
12. Pokorná M, Nečas E, Kratochvíl J, Skřípský R, Andriák M, Franěk O. A sudden increase in partial pressure end-tidal carbon dioxide (PETCO₂) at the moment of return of spontaneous circulation. *J Emerg Med* 2010;38:614–21.
13. Lui CT, Poon KM, Tsui KL. Abrupt rise of end tidal carbon dioxide level was a specific but non-sensitive marker of return of spontaneous circulation in patient with out-of-hospital cardiac arrest. *Resuscitation* 2016;104:53–8.
14. Davis DP, Sell RE, Wilkes N, et al. Electrical and mechanical recovery of cardiac function following out-of-hospital cardiac arrest. *Resuscitation* 2013;84:25–30.
15. Brinkrolf P, Borowski M, Metelmann C, Lukas RP, Pidge-Küllenberg L, Bohn A. Predicting ROSC in out-of-hospital cardiac arrest using

- expiratory carbon dioxide concentration: is trend-detection instead of absolute threshold values the key. *Resuscitation* 2018;122:19–24.
16. Pellis T, Bisera J, Tang W, Weil MH. Expanding automatic external defibrillators to include automated detection of cardiac, respiratory, and cardiorespiratory arrest. *Crit Care Med* 2002;30:S176–8.
 17. Cromie NA, Allen JD, Navarro C, Turner C, Anderson JM, Adgey AAJ. Assessment of the impedance cardiogram recorded by an automated external defibrillator during clinical cardiac arrest. *Crit Care Med* 2010;38:510–7.
 18. Cromie NA, Allen JD, Turner C, Anderson JM, Adgey AAJ. The impedance cardiogram recorded through two electrocardiogram/defibrillator pads as a determinant of cardiac arrest during experimental studies. *Crit Care Med* 2008;36:1578–84.
 19. Losert H, Risdal M, Sterz F, et al. Thoracic-impedance changes measured via defibrillator pads can monitor signs of circulation. *Resuscitation* 2007;73:221–8.
 20. Risdal M, Aase SO, Kramer-Johansen J, Eftesol T. Automatic identification of return of spontaneous circulation during cardiopulmonary resuscitation. *IEEE Trans Biomed Eng* 2008;55:60–8.
 21. Alonso E, Aramendi E, Daya M, et al. Circulation detection using the electrocardiogram and the thoracic impedance acquired by defibrillation pads. *Resuscitation* 2016;99:56–62.
 22. Ruiz JM, de Gauna SR, González-Otero DM, et al. Circulation assessment by automated external defibrillators during cardiopulmonary resuscitation. *Resuscitation* 2018;128:158–63.
 23. Aramendi E, Elola A, Alonso E, et al. Feasibility of the capnogram to monitor ventilation rate during cardiopulmonary resuscitation. *Resuscitation* 2017;110:162–8.
 24. Ayala U, Eftestøl T, Alonso E, et al. Automatic detection of chest compressions for the assessment of CPR-quality parameters. *Resuscitation* 2014;85:957–63.
 25. Alonso E, Ruiz J, Aramendi E, et al. Reliability and accuracy of the thoracic impedance signal for measuring cardiopulmonary resuscitation quality metrics. *Resuscitation* 2015;88:28–34.
 26. Irusta U, Ruiz J, Aramendi E, de Gauna SR, Ayala U, Alonso E. A high-temporal resolution algorithm to discriminate shockable from nonshockable rhythms in adults and children. *Resuscitation* 2012;83:1090–7.
 27. Elola A, Aramendi E, Irusta U, Del Ser J, Alonso E, Daya M. ECG-based pulse detection during cardiac arrest using random forest classifier. *Med Biol Eng Comput* 2019;57:453–62.
 28. Wei L, Chen G, Yang Z, Yu T, Quan W, Li Y. Detection of spontaneous pulse using the acceleration signals acquired from CPR feedback sensor in a porcine model of cardiac arrest. *PLoS One* 2017;12:e0189217.
 29. Breiman L. Random forests. *Mach Learn* 2001;45:5–32.
 30. Stone M. Cross-validated choice and assessment of statistical predictions. *J R Stat Soc Ser B Methodol* 1974;111–47.
 31. Zou KH, O'Malley AJ, Mauri L. Receiver-operating characteristic analysis for evaluating diagnostic tests and predictive models. *Circulation* 2007;115:654–7.
 32. Ruopp MD, Perkins NJ, Whitcomb BW, Schisterman EF. Youden, Index and optimal cut-point estimated from observations affected by a lower limit of detection. *Biometr J* 2008;50:419–30.
 33. Kolar M, Križmarić M, Klemen P, Grmec Š. Partial pressure of end-tidal carbon dioxide successful predicts cardiopulmonary resuscitation in the field: a prospective observational study. *Crit Care* 2008;12:R115.
 34. Touma O, Davies M. The prognostic value of end tidal carbon dioxide during cardiac arrest: a systematic review. *Resuscitation* 2013;84:1470–9.
 35. Grmec Š, Klemen P. Does the end-tidal carbon dioxide (EtCO₂) concentration have prognostic value during out-of-hospital cardiac arrest? *Eur J Emerg Med* 2001;8:263–9.
 36. Weiser C, Poppe M, Sterz F, et al. Initial electrical frequency predicts survival and neurological outcome in out of hospital cardiac arrest patients with pulseless electrical activity. *Resuscitation* 2018;125:34–8.
 37. Skjeflo GW, Nordseth T, Loennechen JP, Bergum D, Skogvoll E. ECG changes during resuscitation of patients with initial pulseless electrical activity are associated with return of spontaneous circulation. *Resuscitation* 2018;127:31–6.
 38. Elola A, Aramendi E, Irusta U, et al. ECG characteristics of pulseless electrical activity associated with return of spontaneous circulation in out-of-hospital cardiac arrest. *Resuscitation* 2018;130:e54.
 39. Prosen G, Križmarić M, Završnik J, Grmec Š. Impact of modified treatment in echocardiographically confirmed pseudo-pulseless electrical activity in out-of-hospital cardiac arrest patients with constant end-tidal carbon dioxide pressure during compression pauses. *J Int Med Res* 2010;38:1458–67.
 40. Raimondi M, Savastano S, Pamploni G, Molinari S, Degani A, Belliato M. End-tidal carbon dioxide monitoring and load band device for mechanical cardio-pulmonary resuscitation: Never trust the numbers, believe at the curves. *Resuscitation* 2016;103:e9–e10.
 41. Ruiz J, Alonso E, Aramendi E, et al. Reliable extraction of the circulation component in the thoracic impedance measured by defibrillation pads. *Resuscitation* 2013;84:1345–52.